Article

Prediction of the 3D Structure and Dynamics of Human DP G-Protein Coupled Receptor Bound to an Agonist and an Antagonist

Youyong Li, Fangqiang Zhu, Nagarajan Vaidehi, William A. Goddard, Felix Sheinerman, Stephan Reiling, Isabelle Morize, Lan Mu, Keith Harris, Ali Ardati, and Abdelazize Laoui

J. Am. Chem. Soc., **2007**, 129 (35), 10720-10731• DOI: 10.1021/ja070865d • Publication Date (Web): 11 August 2007

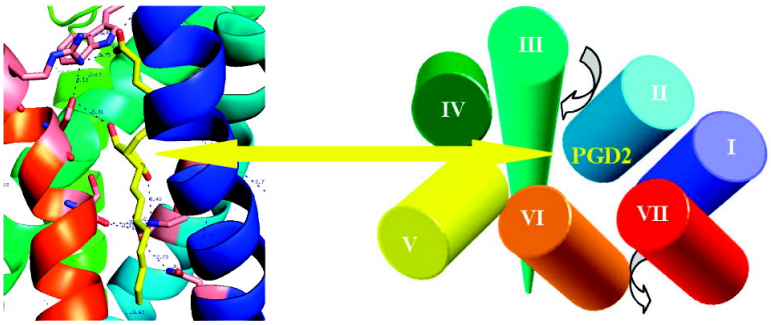

More About This Article

Additional resources and features associated with this article are available within the HTML version:

- Supporting Information
- Access to high resolution figures
- Links to articles and content related to this article
- Copyright permission to reproduce figures and/or text from this article

View the Full Text HTML

J|A|C|S
ARTICLES
Published on Web 08/11/2007

Prediction of the 3D Structure and Dynamics of Human DP G-Protein Coupled Receptor Bound to an Agonist and an Antagonist

Youyong Li,[†] Fangqiang Zhu,[†] Nagarajan Vaidehi,*[,†,‡] William A. Goddard, III,*[,†] Felix Sheinerman,[§] Stephan Reiling,[§] Isabelle Morize,[§] Lan Mu,[§] Keith Harris,[§] Ali Ardati,[§] and Abdelazize Laoui[§]

Contribution from the Materials and Process Simulation Center (MC 139-74), California Institute of Technology, Pasadena, California 91125, and Sanofi-Aventis Pharma, Bridgewater, New Jersey 08807-0800

Received February 13, 2007; E-mail: wag@wag.caltech.edu; NVaidehi@coh.org

Abstract: Prostanoids play important physiological roles in the cardiovascular and immune systems and in pain sensation in peripheral systems through their interactions with eight G-protein coupled receptors. These receptors are important drug targets, but development of subtype specific agonists and antagonists has been hampered by the lack of 3D structures for these receptors. We report here the 3D structure for the human DP G-protein coupled receptor (GPCR) predicted by the MembStruk computational method. To validate this structure, we use the HierDock computational method to predict the binding mode for the endogenous agonist (PGD2) to DP. Based on our structure, we predicted the binding of different antagonists and optimized them. We find that PGD2 binds vertically to DP in the TM1237 region with the α chain toward the extracellular (EC) region and the ω chain toward the middle of the membrane. This structure explains the selectivity of the DP receptor and the residues involved in the predicted binding site correlate very well with available mutation experiments on DP, IP, TP, FP, and EP subtypes. We report molecular dynamics of DP in explicit lipid and water and find that the binding of the PGD2 agonist leads to correlated rotations of helices of TM3 and TM7, whereas binding of antagonist leads to no such rotations. Thus, these motions may be related to the mechanism of activation.

1. Introduction

Prostanoids (prostaglandins (PG) and thromboxanes (TX), both metabolites of arachidonic acid)[1,2] play important physiological roles in the cardiovascular and immune systems and in pain sensation in peripheral systems. They exert a variety of actions in the body through binding to specific cell surface prostanoid receptors. The eight subtypes of prostanoid receptors all belong to the family A of G-protein coupled receptors (GPCRs). Various prostanoids exert their activity preferentially through prostanoid receptors. For example, the DP receptor preferentially binds prostaglandin PGD2 with substantially more affinity than any of the other prostanoid ligands, and PGD2 shows quite a preference to DP receptor with diminished activity on EP3 and no activity on the other prostanoid receptors.[1] This extensive heterogeneity and preference of the prostanoid receptors is reflected by the remarkable diversity of physiological effects that can be elicited by prostanoids.

Perhaps the most well-known of these effects are those that produce pain, fever, and inflammation, which can be relieved through the inhibition of COX-1 or COX-2 by aspirin and nonsteroidal anti-inflammatory drugs (NSAIDs).[3,4] Other important effects of the prostanoids involve the vascular, reproductive, bone, and immune systems.[1] Specifically, PGD(2) functions as a mast cell-derived mediator to trigger asthmatic responses.[5]

The development of subtype-specific agonists and antagonists has been hampered by the lack of 3D structures for prostanoid receptors. As a first step in providing a structural basis for understanding the activity and selectivity of these receptors, we used the MembStruk computational procedure[6−14] to predict the

[†] California Institute of Technology.
[‡] Present address: Division of Immunology, Beckman Research Institute of City of Hope, 1500, Duarte Road, Duarte, CA 91010.
[§] Sanofi-Aventis Pharma.

(1) Narumiya, S.; Sugimoto, Y.; Ushikubi, F. *Physiol. Rev.* **1999**, *79*, 1193.
(2) Breyer, R. M.; Bagdassarian, C. K.; Myers, S. A.; Breyer, M. D. *Annu. Rev. Pharmacol. Toxicol.* **2001**, *41*, 661.
(3) Marnett, L. J.; DuBois, R. N. *Annu. Rev. Pharmacol. Toxicol.* **2002**, *42*, 55.
(4) Subbaramaiah, K.; Dannenberg, A. J. *Trends Pharmacol. Sci.* **2003**, *24*, 96.
(5) Matsuoka, T.; Hirata, M.; Tanaka, H.; et al. *Science* **2000**, *287*, 2013.
(6) Hall, S. E.; Floriano, W. B.; Vaidehi, N.; Goddard, W. A., III. *Chem. Sens.* **2004**, *29*, 595.
(7) Floriano, W. B.; Vaidehi, N.; Goddard, W. A., III. *Chem. Sens.* **2004**, *29*, 269.
(8) Kalani, M. Y.; Vaidehi, N.; Hall, S. E.; Trabanino, R.; Freddolino, P.; Kalani, M. A.; Floriano, W. B.; Kam, V.; Goddard, W. A., III. *Proc. Natl. Acad. Sci.* **2004**, *101*, 3815.
(9) Freddolino, P.; Kalani, M. Y.; Vaidehi, N.; Floriano, W.; Hall, S. E.; Trabanino, R.; Kam, V. W. T.; Goddard, W. A. *Proc. Natl. Acad. Sci.* **2004**, *101*, 2736.
(10) Trabanino, R.; Hall, S. E.; Vaidehi, N.; Floriano, W.; Goddard, W. A. *Biophys. J.* **2004**, *86*, 1904.
(11) Hummel, P.; Vaidehi, N.; Floriano, W. B.; Hall, S. E.; Goddard, W. A., III. *Protein Sci.* **2005**, *14*, 703.
(12) Peng, J.; Vaidehi, N.; Hall, S.; Goddard, W. A., III. *Chem. Med. Chem.* **2006**, *1*, 878.

 10.1021/ja070865d CCC: $37.00

```
Nte: (1)MKSPFYRCQNTTSVE(15)
TM1: (16)KGNSAVMGGVLFSTGLLGNLLALGLLARS(44)
IC1: (45)GLGWCSRRPLRPLP(58)
TM2: (59)SVFYMLVCGLTVTDLLGKCLLSPVVLAAYAQNRS(92)
EC1: (93)LRVLA(97)
TM3: (98)PALDNSLCQAFAFFMSFFGLSSTLQLLAMALECWLSLG(135)
IC2: (136)HPFFYRRHITLRL(148)
TM4: (149)GALVAPVVSAFSLAFCALPFMGFGKF(174)
EC2: (175)VQYCPGTWCFIQMVHEEGSLS(195)
TM5: (196)VLGYSVLYSSLMALLVLATVLCNLGAMRNL(225)
IC3: (226)YAMHRRLQRHPRSCTRDCAEPRADGREASPQPLEE(260)
TM6: (261)LDHLLLLALMTVLFTMCSLPVIYRAYYGAFKDVK(294)
EC3: (295)EKNRTSEEAED(305)
TM7: (306)LRALRFLSVISIVDPWIFIIFRSPV(330)
Cte: (331)FRIFFHKIFIRPLRYRSRCSNSTNMESSL(359)
```

Figure 1. The TM regions and EC, IC loops of human DP receptor predicted using TMPred.

structure for the human DP receptor starting from its amino acid sequence. Then, we used the HierDock computational procedure[15−20] to predict the binding site for endogenous agonist PGD2 with human DP receptor. The details for these predictions are in section 2. Then, we carry out molecular dynamics in explicit lipid and water to check the binding effect on the protein structure. Finally, we report docking results of antagonist based on our structure.

2. Methods

We predicted the three-dimensional structure of DP using MembStruk4.1 computational method summarized here.

2.1. Prediction of the TM Regions and Hydrophobic Centers. The TM regions were predicted using TM2ndS method described in ref 10. The input to TM2ndS method was the 43 sequences of prostanoid receptors from various species. Multiple sequence alignment of the 43 sequences was performed using clustalW. Using the multiple sequence alignment as input, the TM regions were predicted using TM2ndS procedure.[10] The hydrophobic maximum was chosen as the central residue (referred to as the centroid) for each helix that divides the area under the hydrophobicity curve equally. The centroid for each helix is positioned to be in the same *xy* plane (the midpoint of the lipid).**2.2. Prediction of the 3D Structure.** On the basis of the predicted TM regions and the TM centroids, the MembStruk program was used to build and optimize the 3D structure for the human DP receptor. The steps of MembStruk and the predicted structure are described below.

2.2.1. Helix Packing. First, canonical α-helices were built for each TM domain. These α-helix structures were then bundled together as follows. The predicted helix centroid is placed on the *xy* plane using *x*,*y* coordinates on the basis of the low-resolution (7.5 Å) electron density map of frog rhodopsin. The orientation of each helix about its *z*-axis (the χ angle) is chosen so that its helical face with the maximum hydrophobic moment points outward to contact the lipid. In this analysis, we calculate the hydrophobic moment over the full helix but include only the half of the residues that would face outward. Then, each helix is tilted about the point at which the central axis intersects the *xy* plane to match the tilt angles (θ,φ) from frog rhodopsin.

2.2.2. Helix Bending. Next, molecular dynamics (MD) simulations were performed (200 ps) for each individual helix, allowing the helix to attain its equilibrium structure (in some cases it bends or kinks). Then, we chose the structure with the lowest potential energy for each helix and assembled it back into the bundle so that the average axis coincides with the original axis. The side chains were then optimized using SCWRL,[21,22] and the total energy was minimized (conjugate gradients).

2.2.3. RotMin. This initial packed structure was minimized, and then we allowed the individual packing interactions to optimize as follows. Each helix was independently rotated (χ) by $+5°$ and $-5°$, the side chains were repositioned using SCWRL, and then all atoms of the bundle were optimized. If either new angle was lower, it was selected.

2.2.4. Lipid Insertion. At this point, we inserted the seven-helix bundle into a lipid framework ending up with 48 lipids molecules arranged as a bilayer. These lipid molecules were optimized using rigid body dynamics.

2.2.5. RotScan. Starting from the final RotMin structure, we performed a full 360-degree rotational scan (χ) on each of the helices in 5° increments. For each angle, the side chains were reassigned with SCWRL, and the full bundle was reminimized. Multiple minima based on energy and interhelical hydrogen bonds were chosen for each helix. Combination of multiple minima for each helix leads to an ensemble of conformations which were then sorted by the number of interhelical hydrogen bonds and then by total energy.

2.3. Prediction of the Extracelluar (EC) and Intracellular (IC) Loop Structure. We took the best structure from the previous step and added the three EC and IC loops. We expect the three EC and the three IC loops of human DP to be quite flexible and strongly affected by the solvent, which is treated only implicitly in MembStruk. Thus, to provide initial loop structures for our MD studies of the DP receptor, we used the alignment of DP with bovine rhodopsin and then homology threaded the DP loops to the crystal structure (1L9H.pdb). Then, we carried out minimization and dynamics on the loops with fixed helix bundle atoms.

In the crystal structure of bovine rhodopsin, the ECII loop (connecting TM4 and TM5) is closed over the 7-TM barrel, contributing to the binding of 11-*cis*-retinal. This ECII loop has a disulfide bond to TM3 (C105−C183), which is highly conserved among the rhodopsin superfamily of GPCRs. Thus, we include this disulfide bond in our loop structures. It is generally believed that the disulfide bond plays critical role in the folding of seven helices and in the closing of the ECII loop over the 7-TM barrel.[23] Since the rhodopsin in the crystal study is in the inactive form, it is possible that substantial changes occur in ECII and in other loops upon activation.

2.4. Molecular Dynamics Simulation. Since the description of lipid and water in MembStruk is implicit with a skimpy layer of lipid bilayer, we performed molecular dynamics (MD) simulations of the predicted structure of DP receptor with and without ligand for 1∼2 ns in explicit lipid bilayer and water. We carried out MD simulations using NAMD including explicit water and a periodically infinite lipid to determine the interactions of the protein with lipid and water.[14]

We started with the predicted hDP structure, stripped away the lipid molecules, and inserted it in a periodic structure of 1-palmytoil-2-oleoyl-sn-glycero-3-phosphatidylcholine (POPC). In this process, we eliminated lipid molecules within 5 Å of the protein. Then, we inserted this

(13) Vaidehi, N.; Schlyer, S.; Trabanino, R.; Kochanny, M.; Abrol, R.; Koovakat, S.; Dunning, L.; Liang, M.; Sharma, S.; Fox, J. M.; Floriano, W. B.; Mendonça, F. L. d.; Pease, J. E.; Goddard, W. A., III; Horuk, R. *J. Biol. Chem.* **2006**, *281*, 27613.
(14) Spijker, P.; Vaidehi, N.; Freddolino, P.; Hilbers, P.; Goddard, W. *Proc. Natl. Acad. Sci.* **2006**, *103*, 4882.
(15) Datta, D.; Vaidehi, N.; Floriano, W. B.; Kim, K. S.; Prasadarao, N. V.; Goddard, W. A., III. *Proteins: Struct., Funct., Genet.* **2003**, *50*, 213.
(16) Floriano, W. B.; Vaidehi, N.; Zamanakos, G.; Goddard, W. A., III. *J. Med. Chem.* **2004**, *47*, 56.
(17) Datta, D.; Vaidehi, N.; Zhang, D.; Goddard, W. A., III. *Protein Sci.* **2004**, *13*, 2693.
(18) Cho, A.; Wendel, J. A.; Vaidehi, N.; Kekenes-Huskey, P. M.; Floriano, W. B.; Maiti, P. K.; Goddard, W. A., III. *J. Comp. Chem.* **2005**, *26*, 48.
(19) McClendon, C.; Vaidehi, N.; Kam, V.; Zhang, D.; Goddard, W. *Protein Eng. Des. Selection* **2006**, *19*, 195.
(20) Gama, C.; Tully, S.; Sotogaku, N.; Clark, P.; Rawat, M.; Vaidehi, N.; Goddard, W.; Nishi, A.; Hsieh-Wilson, L. C. *Nat. Chem. Biol.* **2006**, *2*, 467.
(21) Canutescu, A.; Shelenkov, A.; Dunbrack, R. *Protein Sci.* **2003**, *12*, 2001.
(22) Altschul, S. F.; Gish, W.; Miller, W.; Myers, E. W.; Lipman, D. J. *J. Mol. Biol.* **1990**, *215*, 403.
(23) Palczewski, K.; Kumasaka, T.; Hori, T.; Behnke, C.; Motoshima, H.; Fox, B.; Trong, I.; Teller, D.; Okada, T.; Stenkamp, R.; Yamamoto, M.; Miyano, M. *Science* **2000**, *289*, 739.

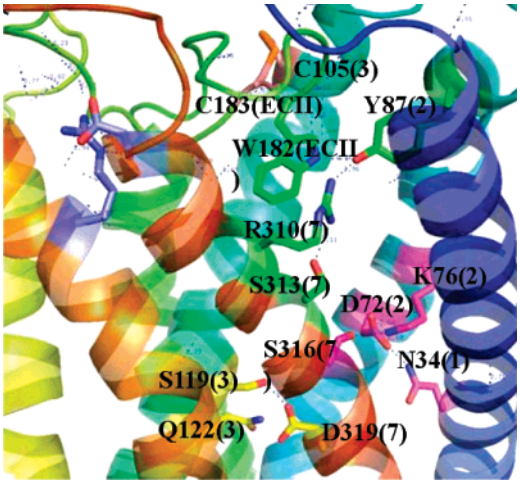

Figure 2. Predicted 3D structure of human DP receptor from MembStruk. (Residues forming interhelical H-bonds are highlighted here.)

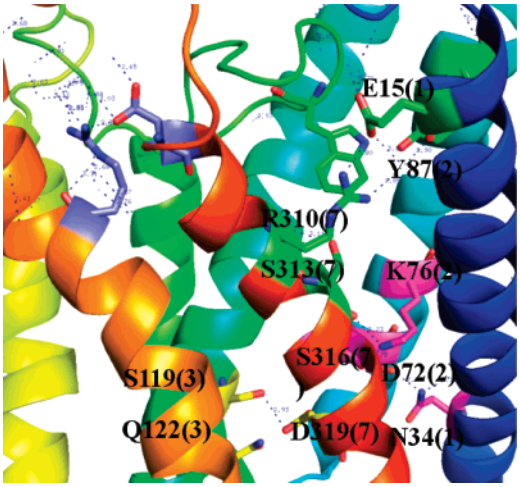

Figure 3. 3D structure of human apo-DP receptor after 1 ns MD with lipid and water (residues forming interhelical H-bonds are highlighted and they are stable during 1 ns MD).

in a box of water molecules and eliminated waters within 5 Å of the lipid and protein. Then, keeping the protein fixed, we allowed the lipid and water to relax using minimization. Then, we minimized the whole system before doing dynamics. The full system (Figure 4) contains the hDP protein, 100 lipid molecules, 6617 water molecules, and 15 chlorine ions for a total of 33 347 atoms per periodic cell. The box size is 66 Å by 66 Å by 72 Å. We then used the NAMD program to carry out 1∼2 ns of NPT MD with a bath temperature of 300 K.

2.5. HierDock Method: Scan the Entire DP Receptor for Binding Sites. We used HierDock approach to predict the binding mode of ligand to DP receptor. The first step is to scan all void regions (shown as magenta dots in Figure 8) in the entire DP receptor structure to locate putative binding regions for PGD2. The void region in the entire receptor structure was partitioned into 27 regions, and the HierDock method was used to dock the cyclopentane ring of PGD2 in each box. Here, we examined the best binding sites that have at least 80% buried surface area. This leads to the TM1237 region shown in Figure 8. Subsequently, we docked the entire PGD2 molecule in this putative binding region using the HierDock2.0 method. The large cavity in the TM1237 region arises from the presence of prolines on TM2 and TM7. The proline on TM7 is 100% conserved among the rhodopsin superfamily. The proline on TM2 is highly conserved among prostanoid family except TP and FP, which have a glycine residue before that position. Rhodopsin has two glycines around that position, and the bending angle of TM2 helix is in a shape that makes TM2 helix pack tightly with TM1,3,7 helices.

3. Results and Discussion

3.1. Description of the Predicted Human DP Structure. The DP receptor sequence lacks some of the well-conserved motifs present in class A GPCRs. For example, the DRY motif on TM3 is ECW, the well-conserved Trp on TM4 becomes Leu, the WXP motif on TM6 becomes SXP, and the NPXXY motif on TM7 is a DPWXF in the DP receptor. Thus, we can expect that the DP receptor might have a different set of stabilizing interhelical hydrogen bonds from rhodopsin. The predicted 3D structure of human apo-DP receptor is shown in Figure 2, and the residues forming interhelical H-bonds are highlighted.

We find an interhelical hydrogen bond between N34(1) and D72(2). N34(1) and D72(2) are conserved in the rhodopsin family A including DP, but the conserved Asn of the NPXXY motif in TM7 is a DPWXF motif in the DP receptor. S316(7), which is not a conserved residue, makes a hydrogen bond with the N34(1) and D72(2). D319(7) makes a hydrogen bond with S119(3). D72(2) also forms a strong salt bridge with the K76-(2) on the same helix. K76(2) is a conservative replacement in other prostaglandin receptors except for thromboxane receptors. We also find a hydrogen bond between R310(7) and Y87(2), where R310(7) is conserved across all prostaglandin receptors while Y87 is present only in DP receptors.

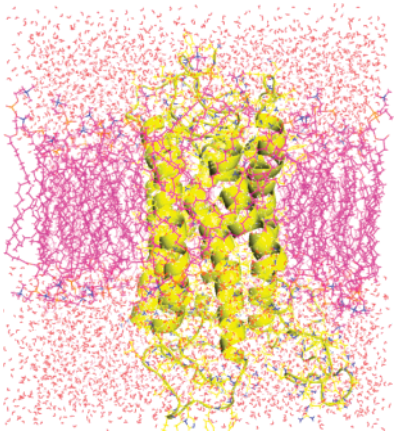

Figure 4. The molecular dynamics simulation box of hDP with lipid and water. Structure after 1 ns of simulation. The EC region is at the top.

3.2. Molecular Dynamics Study of the Predicted Human DP Structure with Lipid and Water. After predicting human apo-DP structure, we performed 1 ns of MD simulations on the apo protein structure.

Figure 3 shows the 3D structure of human DP receptor after 1 ns MD with lipid and water. We find that the protein remains stable during the simulations. Thus, Figure 5 shows that the five important interhelical hydrogen bonds (HB) are all maintained during the 1 ns MD.

Of particular interest is that five water molecules diffuse into binding pocket within the TM regions (Figure 6a), forming water-mediated hydrogen bonds with the buried polar residues. For example, three water molecules cluster around D319(7) with one water molecule around D72(2) and one around S119(3). Thus, the interhelical hydrogen bond between N34(1) and D72-(2) becomes water mediated. Figure 6b shows the time evolution of the distance of these water molecules to the polar residues. The rhodopsin X-ray structure also showed some water mol-

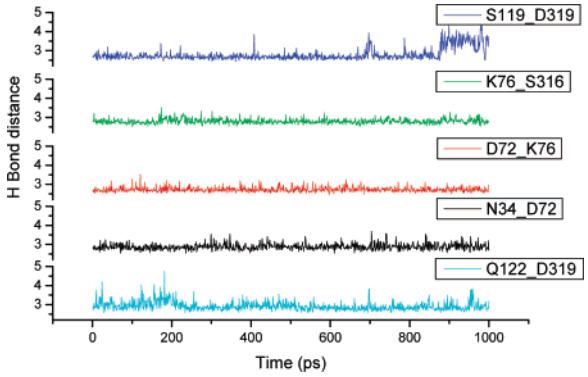

Figure 5. The stability of the predicted hydrogen bonds (HB) in hDP over 1 ns of MD with full lipid and water. This shows that the hydrogen bonds are conserved during MD.

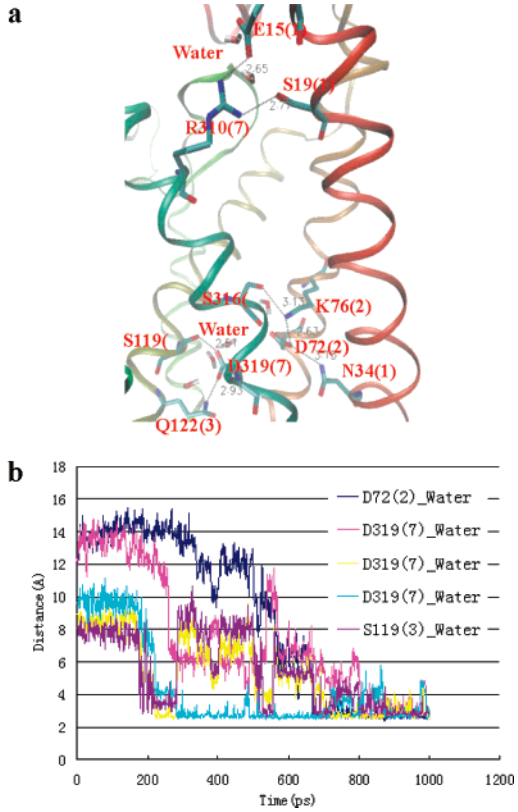

Figure 6. (a) 3D structure of human apo-DP receptor after 1 ns MD with lipid and water (water and residues forming interhelical hydrogen bonds are highlighted). (b) The final structure for hDP finds five waters in the binding site. This shows the evolution of the distance of the waters to the hydrophilic residues in the pocket.

ecules sufficiently strongly bound to be observed,[24] which were observed in the vicinity of highly conserved residues and have been suggested to regulate the activity of rhodopsin-like GPCRs.

Figure 7a shows the root mean square deviation (rmsd) time evolution of the helical segments during the 1 ns MD. Here, rmsd is with respect to the last frame of the 1 ns trajectory. The total rmsd's range from the initial predicted structure to the final one in the trajectory ranges for 1.5−2.3 Å. Focusing on the last 200 ps, these fluctuations range from 1.0 Å to 1.5 Å, except TM5 which reaches 2.0 Å.

(24) Okada, T.; Fujiyoshi, Y.; Silow, M.; Navarro, J.; Landau, E. M.; Shichida, Y. *Proc. Natl. Acad. Sci.* **2002**, *99*, 5982.

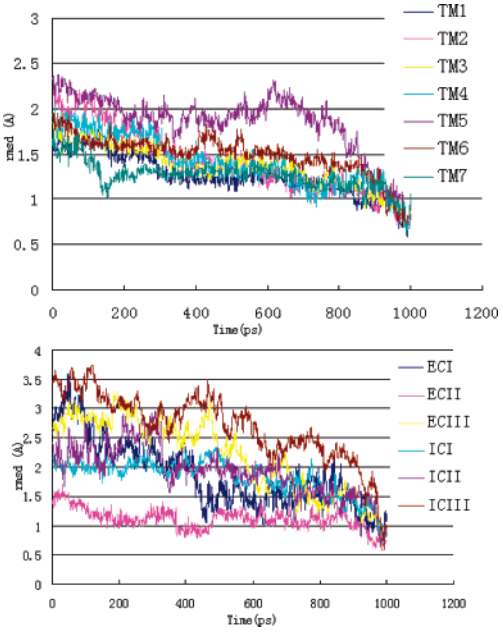

Figure 7. Rmsd evolution of each helix and loop during 1 ns molecular dynamics (the reference is the last frame). ECII is rigid because of the disulfide linkage with TM3.

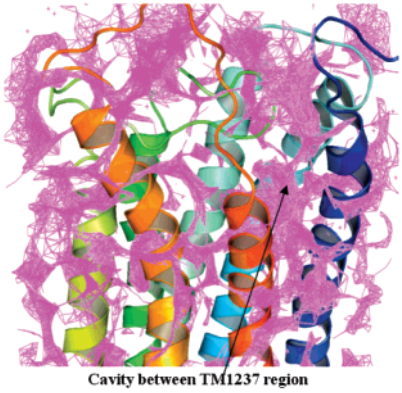

Figure 8. Void regions of the human DP receptor from a scan using the cyclopentane ring of PGD2. Spheres are shown in magenta dots. The best binding site is obtained in the TM1237 region.

Figure 7b shows the time evolution of the loop segments. Larger movements are observed for the loops, with fluctuations ranging from 1.5 Å for ECII (the most rigid loop because of the disulfide linkage with TM3) to 3.5 Å for ICIII. Focusing on the last 200 ps, we find fluctuations of 1.0 Å for ECII and 2.3 Å for ICIII.

3.3. Predicted Binding Site of Prostanoid Compounds in the Predicted DP Structure. The predicted binding site of PGD2 is shown in Figure 9a. PGD2 is located between the TM 1, 2, 3, and 7 helices and is covered by the ECII loop.

We find favorable hydrophobic interactions of the α chain with L26(1) and F27(1). The α chain of PGD2 points up toward the EC region with the ω chain pointing down between TM1 and TM7. The critical elements of bonding are the following:

(1) The carboxylic acid interacts with R310(7).

(2) The carbonyl on the cyclopentane ring of PGD2 has a hydrogen bond with K76(2).

(3) The hydroxyl on the ω chain interacts with S316(7) and K76(2).

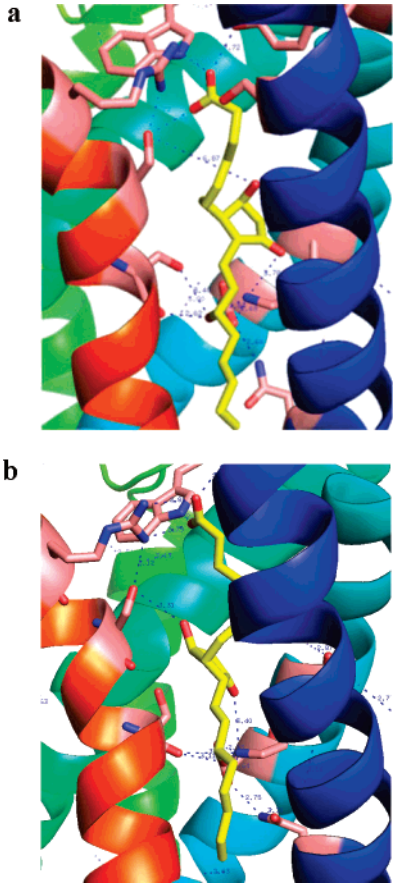

Figure 9. (a) Initial predicted binding site of PGD2 in the DP structure. (b) The final binding site after 2 ns MD with lipid and water. The essential elements of the binding mode are retained but additional favorable interactions are found.

(4) Our predicted structure had no hydrogen bond between S313(7) and 9-OH on the cyclopentane ring of PGD2. However, in the MD simulations we find that a hydrogen bond forms between S313(7) and 9-OH.

(5) A hydrophobic pocket surrounds the α chain with M22-(1), G23(1), Y87(2), W182(ECII), L309(7), R310(7), L312(7), and S313(7) within 6 Å.

(6) A hydrophobic pocket surrounds the ω chain with L26-(1), G30(1), I317(7), P320(7), and W321(7) within 6 Å.

3.4. Molecular Dynamics Study of the Complex of hDP-PGD2 with Lipid and Water. After inserting the predicted PGD2/hDP complex into the infinite lipid membrane and solvating fully with water (using the procedure described in section 2.4), we performed 2 ns of MD. Figure 9 compares the structure of the complex after 2 ns molecular dynamics with the initial predicted structure. We find that the three hydrogen bonds of the original predicted structure remain stable during 2 ns dynamics. However, one additional H-bond is formed between 9-OH group of PGD2 and S313(7).

Figure 10 shows the time evolution for the hydrogen bond distances between PGD2 and hDP.

(1) 15-OH−S316(7): the hydrogen bond distance remains mostly between 2.9 and 3.1 Å with occasional extensions to 3.8 Å. For the apo protein, S316 was hydrogen bonded to K76(2).

(2) 1-COOH−R310(7): the salt bridge distance is ∼3.0 Å for most the time with occasional extensions to 4.0 Å.

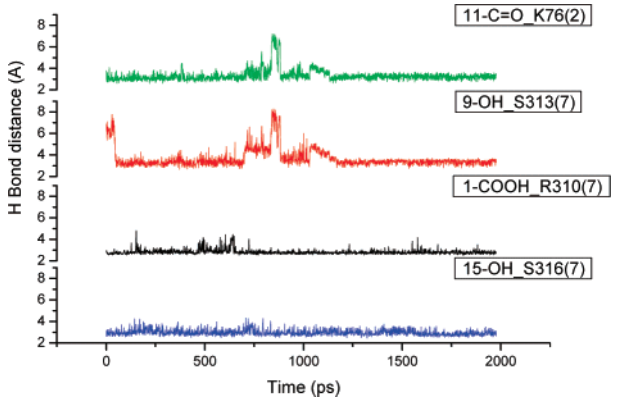

Figure 10. The H-bond distances bonding PGD2 to hDP remain stable during the 2 ns molecular dynamics with lipid and water. Note in particular the formation of the 9-OH−S313(7) hydrogen bond not present in the original predicted structure. The 1-COOH−R310(7) and 15-OH−S316(7) anchors remain stable. We see more fluctuations in the interactions of the cyclopentane ring with some breaking and forming of hydrogen bonds to TM2 and TM7. This is related to the fluctuation of hydrogen bond between K76(2) and S316(7) as shown in Figure 11 and the activation of the receptor.

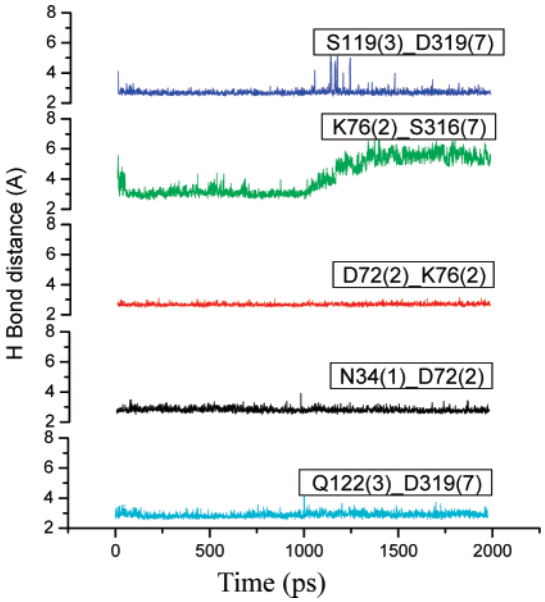

Figure 11. The interhelical hydrogen bond distances inside hDP remain stable during 2 ns MD with lipid and water except for the hydrogen bond between K76(2) and S316(7). The breakage is the effect of binding ligand, which is presented between TM2 and TM7. The tight hydrogen bonds between TM3 and TM7 during dynamics makes the two helices rotate in a cogwheel pattern as shown in Figure 12.

(3) 11-C═O−K76(2): the HB distance is ∼3.5 Å for most the time with occasional extensions to 4.0 Å and a brief one to 6.5 Å. For the apo protein, K76 was hydrogen bonded to S316-(7)

(4) 9-OH−S313(2): the initial distance is 6 Å, but it quickly contracts to 3.5 Å for half of the trajectory and then bounces between 4.5 Å and 7 Å and finally comes back to 4 Å.

Thus, the agonist has disrupted the K76(2)−S316(7) coupling of the apo protein, leading to the clockwise rotation of TM3 and the counterclockwise rotation of TM7. Thus, the changes in interactions between 9-OH, S313(2) and 11-C═O, K76(2) shown in Figure 10 are probably related to activation of the receptor.

As shown in Figure 11, the four important interhelical hydrogen bonds N34(1)−D72(2), D72(2)−K76(2), D319(7)−

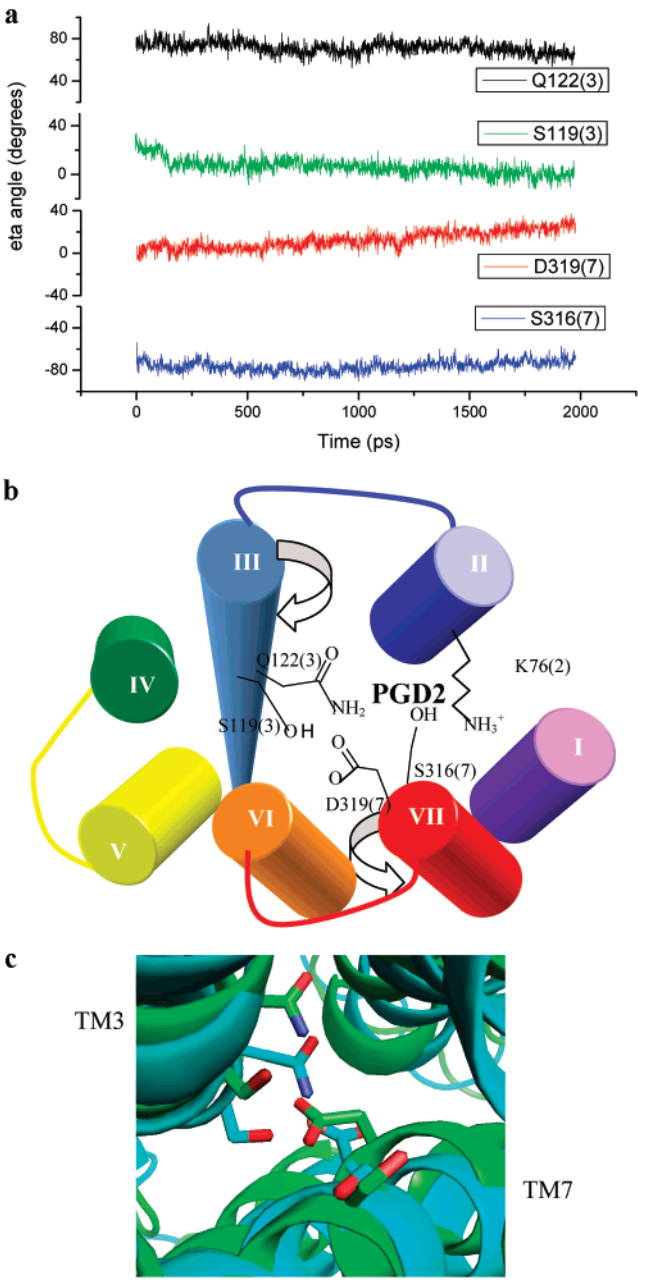

Figure 12. (a) The time evolution of eta angle of TM7 helix and TM3 helix. The eta angle of the residue on the helix is defined by Cα atom, center of helix, center of the whole protein projected to the plane perpendicular to the helix axis. We find that TM7 helix (D319(7) and S316(7)) is rotating anticlockwise and that TM3 helix is rotating clockwise in a cogwheel pattern. In other words, the eta angles of D319(7) and S316(7) are increasing. The eta angles of Q122(3) and S119(3) are decreasing. (b) The schematic representation of the rotation of TM7 helix and TM3 helix upon binding of PGD2. (c). The structure of TM3 and TM7 before MD and after MD with PGD2 bound. Q122(3), S119(3), D319(7), and S316(7) are colored in green and light blue for before MD and after 2 ns MD, respectively.

S119(2), and Q122(3)− D319(7) are rather rigid, remaining between 2.8 Å to 3.0 Å, while the fifth one K76(2)−S316(7) starts at ∼4 Å, drops to 3.2 Å for 1 ns, and finally increases rapidly to ∼5.5 Å. The decoupling between K76(2) and S316(7) occurs because of the binding of 15-OH of PGD2 to S316(7) and of 11-C═O to K76(2).

The eta angle evolution in Figure 12a shows that over the 2 ns of trajectory, TM7 helix (D319(7) and S316(7)) is rotating anticlockwise and TM3 helix is rotating clockwise in a cogwheel pattern as shown in Figure 12b. Figure 12c aligned the structure of TM3 and TM7 before MD and after 2 ns MD.

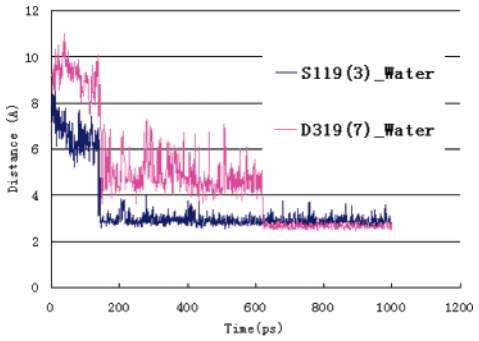

Figure 13. After 1 ns MD, we find two waters in the binding site for PGD2/hDP, which are close to S119(3) and D319(7).

Thus, we conclude that PGD2 forms strong interactions with both TM2 and TM7. The binding of ligand between TM2 and TM7 breaks the strong coupling between TM2 and TM7. This then induces a rotation of TM7. Because of the strong coupling of TM7 with TM3, this in turn induces a rotation in TM3 as shown in Figure 12. This shows how binding of ligand induces changes in other helices that could in turn lead to activation.

This analysis indicates the function of the conserved D319 on TM7. It is not involved directly in the binding of the ligand. However, it couples with TM3 to likely play a role in the process of activation. Indeed, on the basis of mutation experiments, Satoh et al.[25] concluded that the conserved Asp on TM7 of EP3 is important for activation but not for ligand binding.

Our conclusion that D319(7) is important for the activation is consistent with experiments on rhodopsin.[26] The NPxxY (7) of rhodopsin is analogous to DPW*xy* where $x = I/V$ and $y = F/Y$ in the prostanoid receptors, where the D is 319 for DP. In rhodopsin, the NPxxY (7) and E/DRY (3) motifs provide, in concert, a dual control of the activation structural changes in the photoreceptor.[26]

In addition, fluorescence experiments on rhodopsin during activation show that TM3−TM6 interaction is involved for GPCR activation.[27,28] Our results on DP indicates the role of TM3 in activation but suggest that it is coupled with TM7 rather than TM6. Thus, TM3−TM7 interaction may pass the signal to intracellular part (ECW motif, analogous to DRY of rhodopsin) to activate the receptor.

In addition, with PGD2 bound to DP, we find that two water molecules (Figure 13) move into the active site: one to form hydrogen bond with S119(3) and the other to hydrogen bond to D319(7). The other three water molecules observed to form hydrogen bond with D319 and D72 in apo-hDP are now blocked by the bound PGD2.

3.5. The Hydrophilic Interactions and the Hydrophobic Interactions in the Predicted Binding Mode of PGD2 in DP Receptor. Figure 9 shows the important hydrogen

(25) Satoh, S.; Chang, C.-S.; Katoh, H.; Hasegawa, H.; Nakamura, K.; Aoki, J.; Fujita, H.; Ichikawa, A.; Negishi, M. *Biochem. Biophys. Res. Commun.* **1999**, *255*, 164.
(26) Fritze, O.; Filipek, S.; Kuksa, V.; Palczewski, K.; Hofmann, K. P.; Ernst, O. P. *PNAS* **2003**, *100*, 2290.
(27) Farrens, D.; Altenbach, C.; Yang, K.; Hubbell, W.; Khorana, H. *Science* **1996**, *274*, 768.
(28) Sheikh, S.; Zvyaga, T.; Lichtarge, O.; Sakma, T.; Bourne, H. *Nature* **1996**, *383*, 347.
(29) Kobayashi, T.; Ushikubi, F.; Narumiya, S. *J. Biol. Chem.* **2000**, *275*, 24294.

```
TM1
hDP          KGNSAVMGGVLFSTGLLGNLLALGLLARS
hIP          GSVGPATSTLMFVAGVVGNGLALGILSAR
hEP1          GASPALPIFSMTLGAVSNLLALALLAQA
hEP2         PGESPAISSVMFSAGVLGNLIALALLARR
hEP3         GSVSVAFPITMLLTGFVGNALAMLLVSRS
hEP4         LNSPVTIPAVMFIFGVVGNLVAIVVLCKS
hFP          NRLSVFFSVIFMTVGILSNSLAIAILMKA
hTP          LIASPWFAASFCVVGLASNLLALSVLAGA
TM2
hDP        SVFYMLVCGLTVTDLLGKCLLSPVVLAAYAQN---RS
hIP        SAFAVLVTGLAATDLLGTSFLSPAVFVAYARNSSLLG
hEP1       TTFLLFVASLLATDLAGH--VIPGALVLRLY------
hEP2       SLFHVLVTELVFTDLLGTCLISPVVLASYARN---QT
hEP3       KSFLLCIGWLALTDLVGQLLTTPVVIVVYLS---KQR
hEP4       TTFYTLVCGLAVTDLLGTLLVSPVTIATYMK----GQ
hFP        ASFLLLASGLVITDFFGHLINGAIAVFVYAS---DKE
hTP        SSFLTFLCGLVLTDFLGLLVTGTIVVSQHAALFEWHA
TM3
hDP        PALDNSLCQAFAFFMSFFGLSSTLQLLAMALECWLSLG
hIP        PA----LCDAFAFAMTFFGLASMLILFAMAVERCLALS
hEP1       PA--GGACHFLGGCMVFFGLCPLLLGCGMAVERCVGVT
hEP2       PE--SRACTYFAFAMTFFSLATMLMLFAMALERYLSIG
hEP3       PS--GRLCTFFGLTMTVFGLSSLFIASAMAVERALAIR
hEP4       P-----LCEYSTFILLFFSLSGLSIICAMSVERYLAIN
hFP        QS--NVLCSIFGICMVFSGLCPLLLGSVMAIERCIGVT
hTP        R-----LCRFMGVVMIFFGLSPLLLGAAMASERYLGIT
ECII
hDP        VQYCPGTWCFIQMVHEEGSLS
hIP        QQYCPGSWCFLRMRWAQPGG-
hEP1       ELQYPGTWCFIGLGPPGGWRQ
hEP2       VQYCPGTWCFIRHGR------
hEP3       TVQWPGTWCFISTGRGGNGTS
hEP4       RLQYPDTWCFIDWTTNVTAH-
hFP        KIQASRTWCFYNTEDIKDWED
hTP        TVQYPGSWCFLTLGAESGDVA
TM7
hDP        LRALRFLSVISIVDPWIFIIFRSPV
hIP        LLAFRFYAFNPILDPWVFILFRKAV
hEP1       FLAVRLASWNQILDPWVYILLRQAV
hEP2       LQALRFLSINSIIDPWVFAILRPPV
hEP3       LIAVRLASLNQILDPWVYLLLRKIL
hEP4       LQAIRIASVNPILDPWIYILLRKTV
hFP        LFALRMATWNQILDPWVYILLRKAV
hTP        LIYLRVATWNQILDPWVYILFRRAV
```

Figure 14. Amino acid sequence alignment of eight human prostanoid receptors for TM1, 2, 3, and 7 and ECII. Conserved residues within the prostanoid family are in bold. The residues of DP predicted to make strong hydrogen bonds to PGD2 are in blue while the residues involved in hydrophobic stabilization of the PGD2 are underlined. The residues shown by mutation to be important to binding are highlighted in gray (includes G23(1), K76(2) of DP/IP chimericas;[29] D60(2), S68(2), Y75(2), F95(3), F97(3), F278(7), R279(7) of IP receptor;[30,31] R302(7), L304(7), Thr(ECII) of EP2;[32] W199(ECII), T202(ECII), R329(7) of EP3;[33−35] H81(2);[36,37] R291-(7)[37] of FP; and L291(7), R295(7), W299(7) of TP[38]).

bonds between the agonist PGD2 and hDP. These are the following:

(1) 1-COOH of the α chain with R310(7) and W182(ECII).

(2) 15-OH of the ω chain with S316(7) and K76(2).

(3) 11-C═O of the cyclopentane ring to K76(2)

(4) 9-OH of the cyclopentane ring to S313(7).

In addition, there are favorable hydrophobic channels with residues interacting with the hydrophobic parts of the α and ω chains: α chain with M22(1), G23(1), L26(1), F27(1), V83(2), Y87(2), W182(ECII), L309(7), and L312(7) and ω chain with G30(1), L31(1), S313(7), S316(7), I317(7), P320(7), and W321-(7).

3.6. Contributions to Binding of Each TM Region. Comparison with Mutation Results. 3.6.1. TM7. The residues of TM7 predicted to play a role in hydrogen bonding to PGD2 are R310, S313, and S316, while hydrophobic interactions include L309, L312, I317, P320, and W321.

Particularly important is the salt bridge of R310 with the carboxylic acid part of the α chain of PGD2. Strong evidence in support of this interaction is that mutation of this Arg on IP,[30,31] EP2,[32] EP3,[34,35] FP,[37] and TP[38] leads to significant loss of binding. Such mutation experiments have not yet been carried out for the hDP receptor. S313 and S316 are forming hydrogen bonds with PGD2 in our predicted binding mode. Also, no experiments have been reported for the effect of mutations in S313 or S316 on binding to PGD2. Supporting evidence for interactions of PGD2 with L309 (interacting with the α chain) and R310 is that mutation of the analogous residues F278 and R279 in the IP receptor leads to a dramatic decrease in binding of iloprost[30,31] (wild type, 7.9 nM; F278A, 351.3 nM; R279A, >500 nM).

F311 and V314 face the lipid in our predicted structure and are not involved in binding PGD2. This is consistent with experimental observations for the IP receptor that mutations of the corresponding residues F280 and F283[30,31] do not affect binding (F280A, 10.8nM; F283A, 6.2 nM). We find that L312 of DP interacts directly with the α chain of PGD2. This is consistent with experiments by Kedzie et al.[32] who found that the mutation of the analogous residue L304 of EP2 to Y enhances iloprost potency by ∼100-fold. Although we find R310 to be directly involved in binding, we find that L306 and V314 are close to the bound ligand but do not interact with it directly. This is consistent with experiments by Funk et al.[38] who studied mutation of the analogous residues R295, L291, and W299 on TM7 of TP receptor and showed that W299R, R295Q, and L291F mutations lead to loss of binding to agonist I-BOP. (Four experiments with data not shown in the paper.) Moreover, W299L binds to agonists I-BOP and U-46619.

We find that D319(7) makes a hydrogen bond with S119(3) on TM3 as discussed in section 2 and is not involved in binding to PGD2. D319(7) is 100% conserved among prostanoid receptors and is believed to be important for activation. This aspartic acid residue corresponds to Asn(7) in the NPxxY motif of bovine rhodopsin and might couple with TM2 or TM3 upon signal transduction. Mutation studies on the residue analogous to D319(7) in EP3[25,34] and FP[37] support its expected role for signal transduction and the absence of role in ligand binding.

3.6.2. TM2. K76(2) on TM2 is predicted to hydrogen bond with C═O of the cyclopentane ring of PGD2 and 15-OH hydroxy group on the ω chain of PGD2. K76(2) in turn is also strongly coupled to D72(2) via a salt bridge. We predict that K76(2) is key in distinguishing PGD2 from other prostaglandins. Evidence in favor of this interaction is that the chimera DP_{N-I}/

(30) Stitham, J.; Stojanovic, A.; Merenick, B. L.; O'Hara, K. A.; Hwa, J. *J. Biol. Chem.* **2003**, *278*, 4250.
(31) Stitham, J.; Stojanovic, A.; Ross, L. A.; Blount, A. C.; Hwa, J. *Biochemistry* **2004**, *43*, 8974.
(32) Kedzie, K. M.; Donello, J. E.; Krauss, H. A.; Regan, J. W.; Gil, D. W. *Mol. Pharmacol.* **1998**, *54*, 584.
(33) Audoly, L.; Breyer, R. *J. Biol. Chem.* **1997**, *272*, 13475.
(34) Audoly, L.; Breyer, R. M. *Mol. Pharmacol.* **1997**, *51*, 61.
(35) Huang, C.; Tai, H. H. *Biochem. J.* **1995**, *307*, 493.
(36) Rehwald, M.; Neuschafer-Rube, F.; de Vries, C.; Puschel, G. P. *FEBS Lett.* **1999**, *443*, 357.
(37) Neuschafer-Rube, F.; Engemaier, E.; Koch, S.; Roer, U.; Puschel, G. P. *Biochem. J.* **2003**, *371*, 443.
(38) Funk, C. D.; Furci, L.; Moran, N.; Fitzgerald, G. A. *Mol. Pharmacol.* **1993**, *44*, 934.

IP_{II-EX1}/DP_{III-C}[29,39] recognizes iloprost and not PDG2. Moreover, CR_{T94K} (CR: chimeric receptor) acquires the ability to bind PGD2, Ki 23 nM compared to 11 nM for mDP while retaining its binding to iloprost.

Favorable hydrophobic interactions are provided by S80(2), V83(2), and Y87(2). This is consistent with experiments on the FP receptor, where H81(2)/FP corresponds to K76(2)/DP. Rewald et al.[36] found that substitution of H81(2) of rat FP with several different amino acids led either to a loss of ligand binding or to alterations in the optimum pH for receptor ligand interaction. Moreover, Neuschafer-Rube et al.[37] found that H81A(2) of FP abolishes ligand binding (from 6.4 nM to no binding). Our predicted structure has Q89(2) facing lipid and forming hydrogen bond with the backbone of A85(2) and L96-(ECI). This is consistent with the mutation result that the chimeric receptor CR_{R107Q}[29,39] does not change the binding of PGD2.

Residues L78, V82, L84, A85, and R91 on TM2 of DP lie farther than 6 Å from the bound PGD2 and do not participate directly in binding. L78, V82, L84, and A85 face the lipid, while R91 faces TM1 but is not close to bound PGD2. Y87 covers PGD2, and R91 is one turn above Y87. This is consistent with the observation that CRT94K binds to both PGD2 and iloprost while $CR_{T94K/F96L}$, $CR_{T94K/A100M}$, $CR_{T94K/F102L}$, $CR_{T94K/V103A}$, and $CR_{T94K/S109Q}$[29,39] do not change the binding to PGD2. We observe that S80 and Y87 of DP have favorable hydrophobic interactions with the α chain of PGD2, and evidence in favor of this comes from studies on IP which is the closest prostanoid receptor to DP. Mutations by Stitham and co-workers[30,31] on human prostacyclin receptor of the analogous residues S68A-(2) and Y75A(2) lead to significant change of binding affinity of iloprost (wild type, 7.9 nM; S68A, 62.3 nM; Y75A, >500). We predict that D72(2) couples with 15-OH of PGD2 through K76(2) while also interacting with N34(1). This is consistent with the observation that D72(2) is 100% conserved among all the rhodopsin superfamily while the 15-OH of the ω chain is 100% conserved among all prostanoid compounds. In addition, mutation by Stitham and co-workers[30,31] on human prostacyclin receptor of the corresponding residue D60(2) leads to significant change of binding affinity of iloprost (from 7.9 nM to >500 nM).

3.6.3. TM1. In the predicted structure of the hDP receptor, TM1 provides hydrophobic stabilization to the α chain of PGD2 with M22, G23, L26, F27, G30, L31, and N34. There is limited mutation data on TM1 of prostanoid family receptors. Evidence that G23(1) is directly involved in the binding pocket was provided by Kobayashi and co-workers[29,39] who studied chimeras of the mouse prostaglandin I receptor (mIP) and the mouse prostaglandin D receptor (mDP). mIP recognizes iloprost and PGE1, while mDP recognizes only PGD2. However, the chimera $DP_{N-I}/IP_{II-EX1}/DP_{III-C}$ recognizes only iloprost. CR_{G22S} of the chimera recovers the ability to bind PGE1, PGE2, and PGD2. We find that A19 faces the lipid, close to TM2, and is not involved in binding PGD2. Evidence supporting this is that CR_{A19P}[29,39] does not change the binding of PGD2. L26 and L31 are directly involved in the predicted binding mode, and the chimera $CR_{L25M/L30V}$[29,39] does not bind to PGD2 and iloprost.

3.6.4. TM3. F108, M112, and F115 on TM3 provide hydrophobic stabilization to the α chain and the cyclopentane ring of PGD2. Evidence in favor of this is that Stitham and co-workers[30,31] found that F95A(3) and F97A(3) of IP (corresponding to F108(3) and F110(3) of DP) change the binding affinity of iloprost greater than 10 fold. F108(3) interacts with both the α chain and the ω chain of PGD2 while F110(3) of DP is located between TM2 and TM4, which might play a role in stabilizing the helix bundle.

3.6.5. ECII. We predict that PGD2 is located within the TM1237 region and is covered by the ECII loop. W182 in ECII forms a hydrogen bond to the 1-COOH of PGD2, and T181 is within 6 Å of PGD2. Both T181 and W182 on ECII are conserved among prostanoid family receptors. EP2/EP4 chimera studies by Stillman and co-workers[40,41] show that residues on ECII play a role in ligand binding and that the conserved threonine of ECII is required for iloprost ligand binding. Other studies by Audoly and Breyer[33] who examined binding of EP3 to prostanoid compounds with a C-1 methyl ester show that ECII is involved in prostanoid binding. They found that mutations on ECII $EP3_{W199A}$ and $EP3_{T202A}$ (analogous to C178 and T181 in DP) resulted in increased in affinity of PGE2. Moreover, $EP3_{P200S}$ (analogous to P179 in DP) caused a loss of selectivity <20 fold. These residues are within 6 Å of the ligand in the predicted binding mode.

Ruan and co-workers combined NMR, mutation, and modeling to study loop structure and binding modes of TP and IP.[42,43] They conclude that the ligand could be presented into two binding pockets, ligand recognition pocket (loop region) and TM pocket. This might explain the selectivity of the receptor and it has been shown that the disulfide bond is essential for binding of prostaglandins to TP.[45−47]

3.7. Functional Groups in the Prostanoid Compounds That Confer Selectivity to Prostanoid Receptors. The prediction that the carboxylic acid group of PGD2 interacts with R310-(7) is confirmed strongly by various experiments. The carboxylic acid group and the hydroxyl group on the ω chain are present in all the prostanoid compounds. R310(7) is 100% conserved among prostanoid receptor family and K76(2) is not. Other hydrophobic residues P320(7) and W321(7) interacting with ω chain are also 100% conserved in prostanoid receptor family. Structure activity relationship studies of PGE2 show that the carboxylic acid group and both the ω chain itself and the hydroxyl group in the ω chain are critical for agonist activity.[44] The hydroxyl and carbonyl groups on the cyclopentane ring are not present in all prostanoid compounds, and these groups offer receptor selectivity to the ligand as discussed next.

DP receptor binds to PGD2 and PGD1 with similar affinity and shows at least 2 orders of magnitude lower affinity to other

(39) Kobayashi, T.; Kiriyama, M.; Hirata, T.; Hirata, M.; Ushikubi, F.; Nakamura, K. *J. Biol. Chem.* **1997**, *272*, 15154.
(40) Stillman, B. A.; Audoly, L.; Breyer, R. M. *Eur. J. Pharmacol.* **1998**, *357*, 73.
(41) Stillman, B. A.; Breyer, M. D.; Breyer, R. M. *Mol. Pharmacol.* **1999**, *56*, 545.
(42) Ruan, K.; Wu, J.; So, S.; Jenkins, L.; Ruan, C. *Eur. J. Biochem.* **2004**, *271*, 3006.
(43) So, S.; Wu, J.; Huang, G.; Huang, A.; Li, D.; Ruan, C. *J. Biol. Chem.* **2003**, *278*, 10922.
(44) Ungrin, M. K.; Carriere, M.-C.; Denis, D.; Lamontagne, S.; Sawyer, N.; Stocco, R.; Tremblay, N.; Metters, K. M.; Abramovitz, M. *Mol. Pharmacol.* **2001**, *59*, 1446.
(45) Chiang, N.; Kan, W. M.; Tai, H. H. *Arch. Biochem. Biophys.* **1996**, *334*, 9.
(46) D'Angelo, D. D.; Eubank, J. J.; Davis, M. G.; Dorn, G. W., II. *J. Biol. Chem.* **1996**, *271*, 6233.
(47) Dorn, G. W. I. *J. Biol. Chem.* **1990**, *265*, 4240.

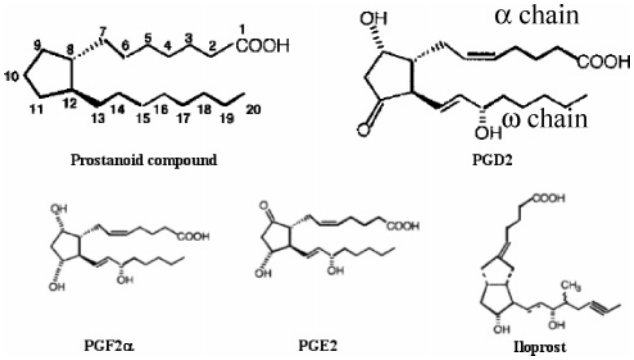

Figure 15. Prostanoid compounds.

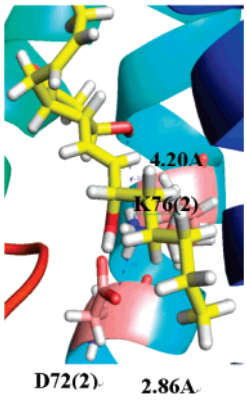

Figure 16. PGE2 bound to hDP. In PGD2, K76(2) couples with both D72-(2) and 11-CO. In PGE2, the 11-OH points away from K76(2), while K76-(2) remains bound to D72(2).

prostanoid compounds. However, the IP receptor binds to PGE1 and PGI analogues (iloprost), but it does not bind PGE2. Assuming that these other prostanoid compounds bind to the hDP receptor in similar binding mode as PGD2, we can explain how the DP receptor prefers PGD2 to other prostanoid compounds like PGF2α, PGE2, and iloprost.

Figure 15 shows the PGD2, PGF2α, PGE2, and iloprost prostanoid compounds along with the numbering convention. The difference among prostanoid compounds is in the functional groups and their location on the cyclopentane ring. The predicted binding site for PGD2/DP has a hydrogen bond of the 11-C═O carbonyl group on the cyclopentane ring to K76(2). K76(2) is only present in DP, and the 11-C═O carbonyl is present only in PGD2. PGF2α, PGE2, and iloprost share the 15-OH hydroxyl group, but they have 11-OH hydroxyl group instead of 11-CO on the cyclopentane ring. More importantly, the 11-position hydroxyl group on PGF2α, PGE2, and iloprost points opposite to the 15-OH hydroxyl group both lying on opposite sides of the plane of the cyclopentane ring. As a result, the 11-OH hydroxyl group does not have a favorable interaction for PGF2α, PGE2, and iloprost with the DP receptor. K76(2) of the DP receptor has a much stronger interaction with PGD2 than PGF2α, PGE2, and iloprost. Figure 16 shows this unfavorable interaction between K76(2) and 11-OH on PGE2. Figure 17 compares the hydrogen bond distance between hDP and PGE2 over 1 ns of MD. This shows that the conserved 1-COOH and 15-OH have stable hydrogen bonds, while the 9-C═O and 11-OH of PGE2 do not form stable hydrogen bonds with hDP receptor.

3.8. Important Residues for Binding. As discussed above, the predicted structure of PGD2/DP is consistent with available experimental results. However, many of these experiments on

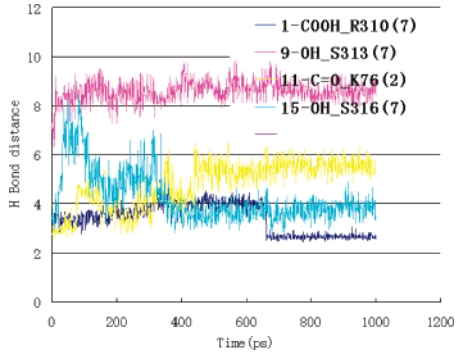

Figure 17. Results from 1 ns simulation of PGE2/hDP. The hydrogen bonds to 1-COOH and 15-OH are stable, while 9-OH and 11-C═O do not form stable hydrogen bonds with hDP receptor.

other prostanoid receptors have not been reported for DP. In addition, our predicted structure suggests several new mutation candidates that can be tested for determining the binding site location of PGD2 on the basis of the predicted model. These include M22(1), G23(1), L26(1), F27(1), G30(1), L31(1), N34-(1), D72(2), K76(2), S80(2), V83(2), Y87(2), F108(3), M112-(3), F115(3), W182(EC2), L309(7), R310(7), L312(7), S313(7), S316(7), I317(7), P320(7), and W321(7).

3.9. Use of the Predicted Structure for Human DP Receptor for Developing New Strongly Bound Antagonists. The motivation in this project sponsored by Sanofi-Aventis was to develop a structure for the DP GPCR protein sufficiently accurate to identify the binding site of antagonists and develop new antagonists with very strong binding affinities. Thus, we considered four classes of lead antagonists, for each of which we predicted the binding sites. Then for each case, we considered ~20 modifications and predicted the binding sites and energies to obtain structure activity relations that could help in determining an optimum drug candidate. One of the optimized compounds is now in preclinical trials at Sanofi-Aventis, on which we will report in due course.

One of the four cases we examined was the cyclopentanoindole (CPI) class of antagonists developed by Merck. Merck recently reported[48,49] the binding constants to human DP receptor for a series of CPI. To illustrate how our predicted human DP structure could be used to optimize new antagonists, we compare here our predicted binding energies for the ligands on which Merck reported binding data.

Our predicted binding mode of the parent CPI is shown in Figure 18, which shows that the carboxylic acid makes a salt bridge to R310(7) and the sulfonyl makes a strong hydrogen bond to K76(2). These are exactly the most important residues in binding the PGD2 agonist to DP. However, CPI does not have the strong interactions with D72(2), S316(7), and S313(7) exhibited by PGD2.

This predicted binding site explains the important interactions of CPI with the receptor. We find four critical regions of binding for the four functional groups, namely: carboxylic acid, cyclopentane ring, indole ring, and benzene ring.

In our predicted structure:

(1) The carboxylic acid interacts with R310(7) and S19(1) along with Y87(2) and W182(ECII).

(48) Sturino, C. F.; Lachance, N.; Boyd, M.; et al. *Bioorg. Med. Chem. Lett.* **2006**, *16*, 3043.
(49) Sturino, C. F.; O'Neill, G.; Lachance, N.; et al. *J. Med. Chem.* **2007**, *50*, 794.

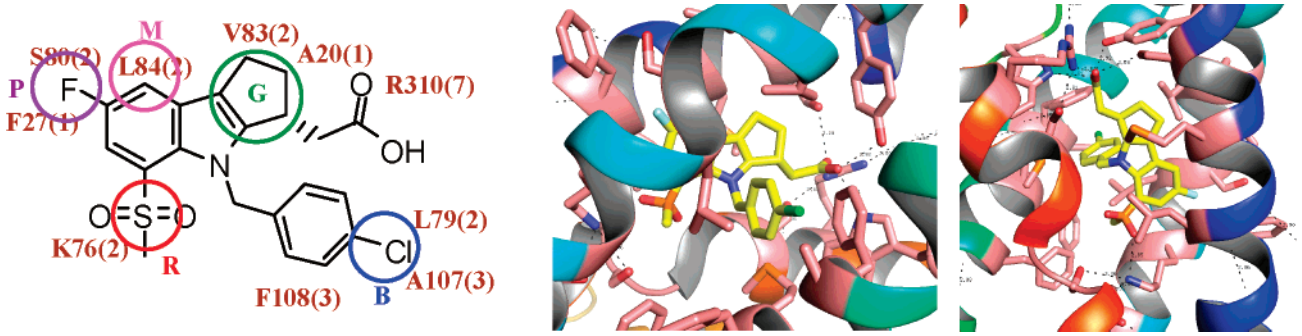

Figure 18. The predicted binding mode of the Merck cyclopentanoindole (CPI) antagonist with human DP receptor.

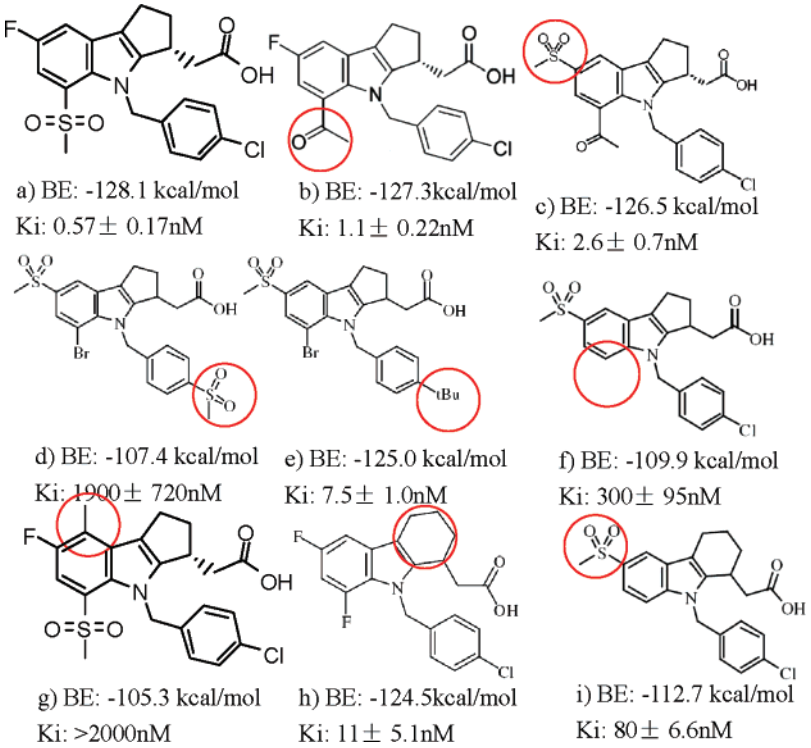

Figure 19. Predicted binding energies of cyclopentanoindole (CPI) and 8 derivatives, compared to the Ki values reported by Merck.[48,49]

(2) The cyclopentane ring is located in a hydrophobic cavity between TM1 and TM2 and interacts with S19(1), A20(1), V83(2), and L84(2).

(3) The indole ring is located in a hydrophobic cavity among TM127 and interacts with L26(1), F27(1), S80(2), V83(2), L84(2), S313(7).

(4) The benzene ring is located between TM2 and TM3, interacting with L79(2), A107(3), and F108(3).

This binding mode of the antagonist CPI is similar to that of the agonist PGD2, described in section 3.3. Most significant is that both PGD2 and CPI bind strongly with K76(2) and R310(7). However, CPI does not interrupt the hydrogen bond network among TM127. As discussed in section 3.3, the agonist PGD2 makes hydrogen bonds with both D72(2) and S316(7), causing a disruption of the coupling between TM2 and TM7, which we suggest is involved in activation. The fact that the antagonist 19a does not disrupt the hydrogen bond network among TM127 is consistent with our hypothesis about activation by the agonist.

Based on our predicted binding mode, we predicted the binding energies of ~20 modified compounds. Eight of these cases are shown in Figure 19.

The CPI derivatives shown in Figure 19 can be partitioned into 5 types of substitutions as highlighted in Figure 18 by circles in various colors: Red (R), Purple (P), Magenta (M), Green (G), and Blue (B). We will now examine these ligands one by one.

(1) 19a→19b (R): The SO_2Me of 19a forms a strong hydrogen bond with K76(2). In 19b, this is replaced with acetyl, which we calculate to decrease the binding by 0.8 kcal/mol. Experimentally the binding decreases by a factor of 2, in excellent agreement with our predictions.

(2) 19b→19c (P): The F in 19b has a strong interaction with S80(2) and F27(1). In 19c, this is replaced with SO_2Me, which we calculate to decrease the binding by 0.8 kcal/mol. Experimentally the binding decreases by a factor of 2.3, in excellent agreement with theory. This result suggests that replacing the fluorine with other small groups might lead to slight improvements.

(3) 19c→19f (R): The acetyl of 19c is replaced with an H in 19f. This loses the strong interaction with K76(2), leading to a predicted decrease in binding of 16.6 kcal/mol, which is consistent with the experimental decrease in binding by a factor of 115. The calculated decrease in binding is much larger than

the observed decrease, probably because there is further rearrangement of the binding site in 19f, which our calculations did not allow.

(4) 19f→19i (G): The cyclopentane ring of 19f is replaced with a cyclohexane ring in 19i. This modifies the interactions with the hydrophobic cavity between TM1 and TM2 [interacting favorably with V83(2) and A20(1)]. We predict an *increase* in binding by 2.8 kcal/mol, which is in excellent agreement with the observed increase in binding by a factor of 2.7.

(5) 19a→19g (M): The hydrogen highlighted in 19a interacts favorably with L84(2), with a distance between this hydrogen to L84(2) (the closest atom) of 3.07 Å, leaving no room for a bigger substituent. Thus substituting the H with methyl to form 19g causes a clash with L84(2), decreasing the binding energy by 22.8 kcal/mol. This indicates that substitution on this position should decrease binding.

(6) 19c→19e (R,B): Fig. 19e differs from 19c by replacing the acetyl with a Br in the R region while simultaneously replacing the Cl in the B region with tBu. We predict that this decreases the binding by 1.5 kcal/mol, which is in excellent agreement with the observed drop by a factor of 2.9. Here the Br interacts favorably with the K76 in the R region. The Cl in the B region interacts with L79(2) and A107(3) and is located in a good hydrophobic cavity between TM2 and TM3. Thus replacing Cl with the tBu is not unfavorable, suggesting that other small hydrophobic groups could be favorable.

(7) 19e→19d (B): Fig. 19d differs from 19e by replacing the tBu group on the phenyl with SO_2Me. We predict that this decreases the binding by 17.6 kcal/mol. The SO_2Me leads to bad interactions with A107(3) and F108(3). This is consistent with the observed drop in binding by a factor of 250. The calculated decrease in binding is much larger than the observed decrease, probably because there is further rearrangement of the binding site in 19d, which our calculations did not allow.

(8) 19b→19h (R,M): Fig. 19h differs from 19b by replacing the cyclopentane in 19b with cyclohexane (which we saw in case 4 is slightly favorable) and replacing the acetyl in 19b with F, which is new. We calculate that the binding decreases by 2.8 kcal/mol, which is consistent with the experimental drop in binding by a factor of 10. Apparently the F is too hydrophobic and/or too small to interact favorable with the K76. The calculated decrease in binding is much larger than the observed decrease, probably because there is further rearrangement of the binding site in 19h, which our calculations did not allow.

Summarizing by the characteristics of the binding site we conclude that

(1) M: leave the H alone, there is no room for improvement (see case 5).

(2) R: Replacing the $MeSO_2$ with F decreases binding by only 0.8 kcal/mol (see case 1) while replacing it with Br may decrease it slightly (case 6 involves two changes with a total decrease by 1.5 kcal/mol). There might be other small ligands that could improve this slightly.

(3) P: Replacing the F with $MeSO_2$ decreases binding by only 0.8 kcal/mol (see case 2). There might be other small ligands that could improve this slightly.

(4) G: replacing the cyclopentane ring with cyclohexane improves binding slightly (2.8 kcal), case 4. Thus, such a change might improve the best ligand, 19a.

(5) B: replacing the Cl with tBu may decrease binding (case 6 involves two changes with a total decrease by 1.5 kcal/mol). There might be other ligands that could improve this slightly.

The above discussion illustrates how the use of the predicted binding site with a comparison of theory and experiment can suggest additional improvements. We include this data here to illustrate the validation and usefulness in having the structure.

Summarizing, we find complete agreement with all reported SAR data on the Merck compounds. Indeed even the cases differing experimentally by only factors of 2 or 3 are predicted correctly in every case. This validates that our predicted 3D human DP receptor is sufficiently accurate to be useful in drug discovery and development.

The above analysis focused only on the binding to the target prostanoid, DP, with no concern for how these ligands might bind to other similar prostanoids. Indeed cross-reactivity is the major problem with designing drugs for GPCRs. It would be quite practical for us to have predicted the structures for the other 7 prostanoid receptors and CRTH (a GPCR that binds to PGD2, but is not actually a prostanoid). With these structures, we could have predicted the binding of the above Merck compounds and optimized them to have maximum binding to DP but minimal binding to the others. We refer to this as the **Infimum GPCR Strategy**. The cost of such an undertaking would be only 2 to 3 million dollars but it could dramatically decrease the likelihood of failure in later trials due to unexpected side effects involving these related receptors.

4. Summary

The 3D structure for the human DP G-protein coupled receptor (GPCR) predicted using the MembStruk computational method leads to features compatible with general understanding of the prostanoid receptors. For example, it has a hydrogen bond coupled triad [Asn34(1), Asp72(2), Ser316(7)] that is conserved among the rhodopsin superfamily of GPCRs and is believed to play a role in activation. We validated the stability of the predicted apo-DP structure with 1 ns of molecular dynamics using an infinite lipid bilayer and explicit water (~33 000 atoms/cell). We found that five water molecules diffuse into the active site region, but the predicted structure and the predicted interhelical interactions are stable.

To further validate this structure, we used the HierDock computational method to predict the binding site and 3D structure for PGD2 (the endogenous agonist) to DP. The predicted binding site positions the PGD2 in a vertical orientation with the α chain toward the extracellular (EC) region and the ω chain toward the middle of the membrane. It has the following interactions: (1) 1-COO^- of PGD2 interacting with R310(7), (2) 15-OH forming hydrogen bond with both S316-(7) and K76(2), (3) 11-C═O interacting with K76(2), and (4) 9-OH forming a hydrogen bond with S313(7).

In addition, hydrophobic cavities from TM1237 surround the hydrophobic parts of the α and ω chains. Thus, PGD2 binds in the TM1237 region and is covered by the ECII loop. We validated the stability of the predicted PGD2/DP structure with 2 ns of MD studies using an infinite lipid bilayer and explicit water (33 000 atoms/cell). We found that two water molecules diffuse into the active site region. Most important, the ligand−protein interactions 9OH-S313(7), 11C═O− K76(2), and 15OH-S316(7) disrupt the coupling of K76(2) and S316(7) in the apo

protein, inducing a clockwise rotation of TM3 and counterclockwise rotations in TM7. In contrast, binding of the antagonist does not disrupt the K76(2)−S316(7) coupling so that no such motion occurs. Thus, these rotations of TM7 and TM3 might be related to activation.

The predicted binding site of PGD2 in hDP explains the variations in experimental activity among various prostanoid compounds to hDP and to mutated versions. In addition, the residues involved in the predicted binding site correlate very well with available mutation experiments on IP, TP, FP, and EP subtypes, providing an understanding of the selectivity of prostanoid receptors. Thus, R310(7), which is 100% conserved among the prostanoid family, recognizes the 1-carboxylic acid on the α chain (also 100% conserved for all prostanoids) and S316(7) (one turn above the conserved proline), which is 100% conserved among the prostanoid family, and recognizes the 15-hydroxyl on the ω chain (also 100% conserved for all prostanoids). In addition, the K76(2) and S313(7) interact with the cyclopentane ring of PGD2 conferring the selectivity of DP receptor. Particularly, K76, which is present only in DP, recognizes the 11-position carbonyl, which is present only in PGD2.

The agreement of the predicted PGD2/DP structure with available experimental data validates the DP and PGD2/DP structures, providing the first atomistic understanding of prostanoid receptors.

To illustrate the value of such structures, we used our predicted structure for the DP receptor to optimize substitutions for different antagonists. Experimental structure−activity relationship (SAR) measurements showed excellent agreement with the predictions, suggesting that the MembStruk protein structures are sufficiently accurate for drug development.

Acknowledgment. Support for the Caltech activities was provided by Sanofi-Aventis Corporation with additional support from NIH (R21-MH073910-01-A1). The computational resources for these studies were provided by grants from ARO-DURIP and ONR-DURIP.

Supporting Information Available: Figure S1 compares the extended and compact structures of the PGD2, both of which were docked to DP (but extended led to the best energy.). Figure S2 shows the changes of the cyclopentane ring between time steps 830 and 870 ps. In addition, complete ref 5, 48, and 49 is given. This material is available free of charge via the Internet at http://pubs.acs.org.

JA070865D